J Mater Sci (2014) 49:8051–8056
DOI 10.1007/s10853-014-8512-9

Buckling of Cu–Zr-based metallic glasses nanowires: molecular dynamics study of surface effects

Javier Wachter · Gonzalo Gutiérrez · Alejandro Zúñiga · Rodrigo Palma

Received: 4 March 2014 / Accepted: 25 July 2014 / Published online: 13 August 2014

Abstract The phenomenon of buckling in $Cu_{45}Zr_{45}Al_{10}$ metallic glass nanowires with different slenderness ratios was studied by means of molecular dynamics simulation. The values of critical stress versus slenderness ratio for two nanowire diameters were obtained. We analyzed the results within the framework of the modified Euler theory of buckling, obtaining values for the surface elastic modulus and the residual surface stress for the two different diameters. Our results show that the $Cu_{45}Zr_{45}Al_{10}$ metallic glass in nanometric size become stiffer and exhibits a lower Young's modulus than that of a bulk sample.

Introduction

Metallic glasses have recently attracted extensive interest due to their unique mechanical and physical properties such as high strength and good corrosion resistance [1, 2]. Their viscosity in the supercooled liquid region, for instance, decreases to such low values that allow the net-shape processing of small-sized, complex parts [3, 4]. Following this line, microelectro-mechanical systems and nanoelectro-mechanical systems (MEMS, NEMS) offer outstanding opportunities for the exploitation of metallic glasses [5], where their high yield strength, low loss coefficient and resilience, and good fatigue resistance are highly desirable. However, to fully exploit the potential of metallic glasses in such applications, more theoretical and experimental studies are still needed. On the other hand, nanostructures—and nanowires in particular—have attracted a growing interest since the last decade due to their extraordinary mechanical, optical, and electrical properties [6, 7]. Unlike their bulk counterparts, these nanostructures owe their properties to a relatively high fraction of highly energetic surface atoms, becoming, therefore, highly size dependent. Among the various properties of interest in nanostructured materials are the mechanical properties. For instance, knowing the stretching, bending, and compression behavior of elements such as nanowires, rods, bars, and plates is an important step toward realizing nanosized structural elements. So far, these elements have been designed using mainly crystalline materials, opening new and exciting opportunities for the use of metallic glasses; however, they will only become a reality if their mechanical response at the nanoscale is better understood.

In this paper, we study the mechanical behavior of metallic glass nanowires under compression by means of molecular dynamics simulations. It is well known that bulk metallic glasses, in addition to the high yield strength and a elastic deformation to a strain limit about 2 % (i.e., more than an order of magnitude greater than conventional crystalline metals), show very little ductility at room temperature [8]. In contrast to their crystalline counterpart, where dislocations are the main carries of plasticity,

J. Wachter (✉)
Departamento de Física, Facultad de Ciencias Naturales, Matemática y del Medio Ambiente, Universidad Tecnológica Metropolitana, Santiago 7800002, Chile
e-mail: javier.wachter@utem.cl

G. Gutiérrez
Departamento de Física, Facultad de Ciencias, Universidad de Chile, Casilla 653, Santiago, Chile

A. Zúñiga
Centro de Engenharia, Modelagem e Ciências Sociais Aplicadas, Universidade Federal do ABC, Santo André, SP 09210-580, Brazil

R. Palma
Departamento de Ingeniería Mecánica, Facultad de Ciencias Físicas Y Matemáticas, Universidad de Chile, Santiago, Chile

metallic glasses (MG) lacked of such coherent, extended defects. As a matter of fact, experiments show that MG does not present a homogeneous deformation regime as in the case of crystalline metals. In general, when a load is applied to a MG sample, after the elastic limit is reached, almost immediately an inhomogeneity appears, the strain being located in a very narrow shear band (thickness about 10–20 nm) and quickly leading to cracking and failure. That is, the bulk metallic glass is brittle. The physics behind this observation has been explained [9] as follows. At the beginning, there exist local regions in the sample prone to undergo shear transformations under loading. These "shear transformations zone" initially act randomly, but gradually they start to correlate both spatially and temporally, forming larger flow zones that give rise a shear band, and then a catastrophic failure. This process proceeds quickly because the enormous elastic energy stored in the uniformly loaded sample.

Interestingly, this picture is different for nanoscopic MG, for instance, thin films or nanowires [10]. In these cases, according the volume of the sample decreases, the energy stored decrease faster than the area associated with the localized shear. Therefore, shear banding proceeds slower and less violent, and the catastrophic failure is suppressed. Homogeneous deformation is the dominant mode. Thus, nanowires seem to be an ideal system to study the onset of plasticity in MG, and it would be interesting to study their behavior under compression, where the phenomenon of buckling could appear. In this case, as we will show in our work, it is important not only to take into account the bulk effects, but also surface effects. The latter, as observed in previous works [11–21], play a crucial role in the evolution dynamics and failure processes of nanowires under compression.

Simulation method

Our model consisted of ternary $Cu_{45}Zr_{45}Al_{10}$ circular cross-sectional amorphous nanowires, ranging from 2000 to 20000 atoms. The nanowires were taken from a well-relaxed bulk metallic glass sample, which was built in the following way. From a 27000 Zr and 27000 Cu atoms B2-type crystalline structure, we randomly replaced Cu and Zr atoms by Al atoms maintaining the 45/45/10 ratio, respectively. Glassy configurations of ternary alloy $Cu_{45}Zr_{45}Al_{10}$ were generated applying the melting-quenching technique to the B2-type crystal model. Using an isothermal–isobaric ensemble with fixed number of particles (NPT ensemble), we heat the samples up to 2000 K temperature and we maintain this temperature by 100 ps. Then, we apply a cooling step to molten CuZrAl, reaching 10 K temperature at a rate of 0.17 K/ps. The obtained bulk metallic glass sample was characterized by using standard techniques [22] such as pair distribution function, coordination number, and the calculation of the elastic modulus. For the latter, we determined a value of $E = 64.4$ GPa by fitting the elastic strain region, in a compression simulation with periodic boundary conditions using a NPT ensemble at strain rate of 10^8 s^{-1} and 10 K of temperature. In Fig. 1, we show the stress–strain curve up to 20 % of strain. The insets show the local atomic strain at $\varepsilon = 0.044$, 0.057, 0.10, and 0.2 strains, as present by the Open VIsualization TOol [28] (OVITO) using the atomic local shear strain scheme [30].

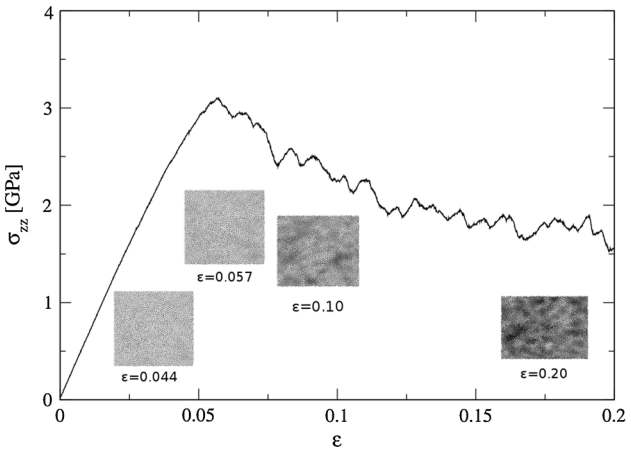

Fig. 1 Stress–strain curve of $Cu_{45}Zr_{45}Al_{10}$ bulk sample in compression. *Insets* show the local atomic strain at different strains

Circular cross sections of amorphous nanowires were constructed by cutting from the $Cu_{45}Zr_{45}Al_{10}$ bulk metallic glass sample. Two sets of nanowires were constructed, ranging from 2000 to 20000 atoms. The first set consists of samples with a fixed cross-sectional diameter of 2.46 nm and ten different length, and second set are samples with a fixed cross-sectional diameter of 3.29 nm and ten different lengths from 9.66 to 96.2 nm. All samples were first relaxed at 10 K for 100 ps in a microcanonical ensemble (NVE ensemble) using temperature rescaling. Then, the samples were relaxed in a NPT ensemble for 100 ps allowing the length of the nanowires to shrink or expand at zero pressure at 10 K. After relaxation, the nanowires were subjected to uniaxial compressive loading.

To simulate the uniaxial compressive tests, both ends of the CuZrAl metallic glass nanowires were clamped. The uniaxial loading was applied at a strain rate of 10^8 s^{-1}. The strain increment was applied on the clamped-boundary atoms, residing within 10 Å at both ends. At each loading step, MD simulations were carried out at 10 K in an NVE ensemble for 1000 simulation steps of relaxation in order to obtain the equilibrium configuration of the nanowires. The simulations are performed using the embedded atom type

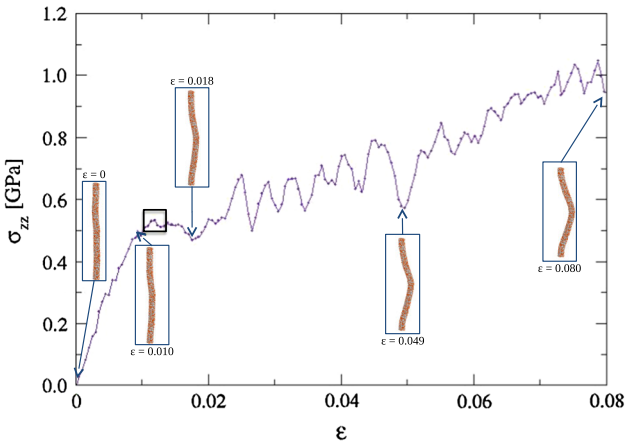

Fig. 2 Stress–strain curve for a $L/D = 16$ nm and $D = 2.46$ nm $Cu_{45}Zr_{45}Al_{10}$ nanowire in compression. *Square* denotes the critical stress and critical strain. *Insets* show atomic model of nanowire at different strains

potentials (EAM) from Cheng et al. [23]. The equations of atomic motion were integrated by the Velocity-Verlet algorithm with a time step of 1.0 fs, using the large-scale atomic molecular massively parallel simulator [24] (LAMMPS) software. For each nanowire, we repeated the loading process with a fixed strain increment at each loading step.

Results and discussion

A typical stress–strain curve resulting from the loading procedure is shown in Fig. 2 for a slenderness of $L/D = 16$ and $D = 2.46$ nm of nanowire diameter. Similar as previous work [25, 26], the stress increases with the increase of strain, and decrease after passing a threshold value, denoted with a square at 1.2 % in this particular case. Then, after further compression, fluctuations appear. That threshold value is regarded in the literature [18, 19, 27] as the critical stress and critical strain point, and it is indicative of the onset of buckling. In fact, in this work, we use that criterion as a definition of the onset of buckling. Of course, the critical value depends on the slenderness of the sample. This procedure is repeated for each of the ten slenderness ratios for each nanowire diameter.

Figure 3 shows the stress–strain simulation at an atomic level for the $L/D = 3.93$ slenderness nanowire, colored according the atomic local shear strain scheme [30] as implemented in Open VIsualization TOol [28] (OVITO). In contrast to what is observed in crystalline materials, where dislocations are generated when plastic deformation begins [29], in our metallic glass simulations, we first observed in Fig. 3b, c the formation of shear transformation zone in the middle of the nanowire, and in Fig. 3d–f then more shear transformation zones coalescing and forming shear bands. Note that instead to have an offset of the nanowire with respect to the axial axis, we can observe that the thickness of shear band increases according as the compression proceed, in agreement to the comments presented in the Introduction. The others nanowires display a similar behavior. Figure 4 shows the stress–strain curves for the ten slenderness ratios of the nanowire with a diameter of 3.28 nm. The critical stress–strain points are denoted with squares. The inset is a zoom of the curve corresponding to a strain between 0.015 and 0.025 and shows how the critical stress increases with the slenderness ratio. This increase is not monotonic due to artifacts in the simulation related to the sample size and deformation rate. The results for the nanowires with a diameter of 2.46 nm present similar behavior.

In order to rationalize our MD simulation results, we employed the Modified Euler (M-Euler) theory proposed by Wang and Feng [31], which relates the critical stress to the slenderness ratio. The M-Euler theory is derived from a modified differential equation of the buckling deformation of a column, which takes into account the influence of the surface elasticity and the residual surface tension. Although there are previous researchers [32, 33] that have employed the traditional Euler theory [34], obvious differences are observed, as pointed out by the results presented by Chen et al. [14] and Ji et al. [35].

According to the M-Euler theory, the critical load of axial buckling of a nanowire is given as follows

$$P_{\mathrm{cr}} = \eta \frac{\pi^2 (\mathrm{EI})^*}{L^2} + H, \tag{1}$$

where L is the effective length of the nanowire and η is a dimensionless constant depending on the support conditions at both ends. $(\mathrm{EI})^*$ is the effective flexural rigidity, which for a circular cross section with diameter D is given by

$$(\mathrm{EI})^* = \frac{1}{64}\pi E D^4 + \frac{1}{8}\pi E_{\mathrm{s}} D^3, \tag{2}$$

where E is the Young's modulus and E_{s} is the surface Young's modulus. H is a constant determined by the residual surface tension τ_0 and the shape of the cross section. For a circular cross section with diameter D, H is given as $H = 2\tau_0 D$. Thus, according to Eqs. (1) and (2), considering that $\eta = 4$ is the value for fixed–fixed support ends, and that $A = \pi(D/2)^2$, the critical stress can be derived as follows

$$\sigma_{\mathrm{cr}} = \frac{P_{\mathrm{cr}}}{A} = \frac{\pi^2 D^2}{4}\left(E + \frac{8E_{\mathrm{s}}}{D}\right)\left(\frac{1}{L}\right)^2 + \frac{8\tau_0}{\pi D}. \tag{3}$$

Therefore, knowing the critical stress with respect to the slenderness ratio allows us to determine E_{s} and τ_0.

Figure 5 shows the main result of our work, which is the variation of the critical stress versus the slenderness ratio

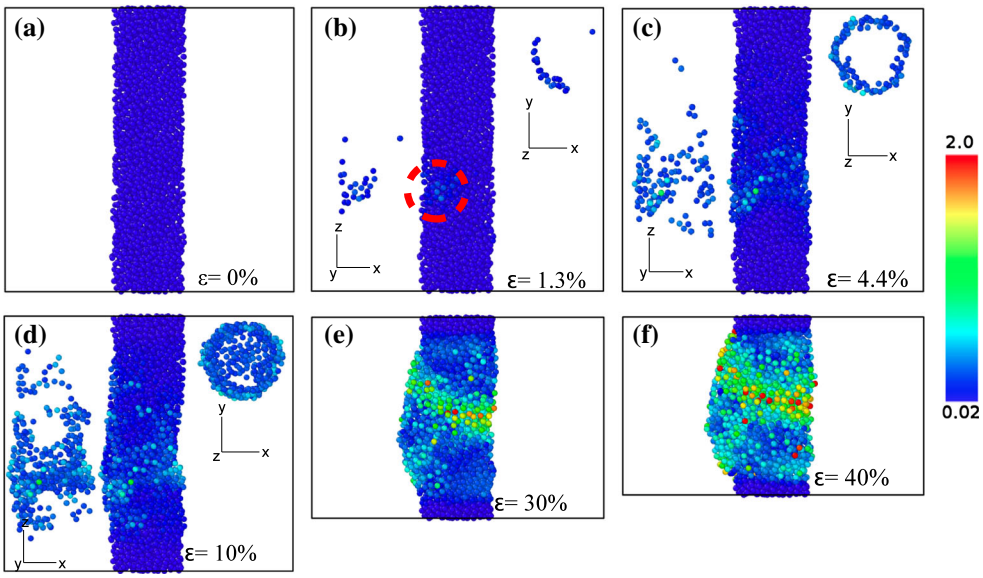

Fig. 3 Local shear strain in $L/D = 3.93$ with $D = 2.46$ nm for the $Cu_{45}Zr_{45}Al_{10}$ metallic glass nanowire atomic model, from **a** zero strain to **f** 40 % of strain. The *dashed-circle* in (**b**) shows the *onset* of a shear transformation zone. In **b**–**d**, the *insets* at the *left* and *right* of the nanowire show the most displaced atoms with respect to their original positions, for a transversal and axial view, respectively

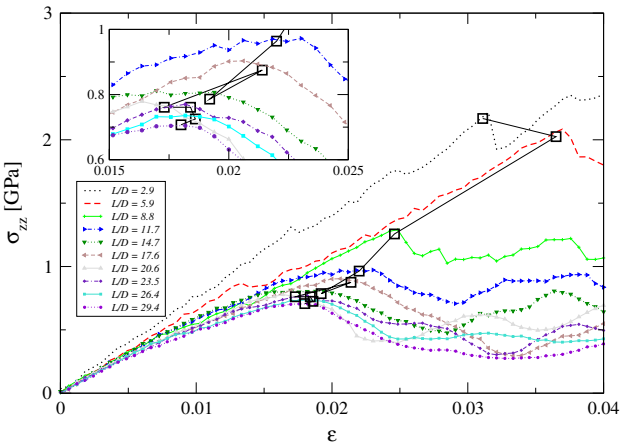

Fig. 4 Stress–strain curves for compressive load ($D = 3.28$ nm, different slenderness ratio). *Squares* indicate the critical stress–strain point. *Solid line* connecting the squares is a guide to the eye

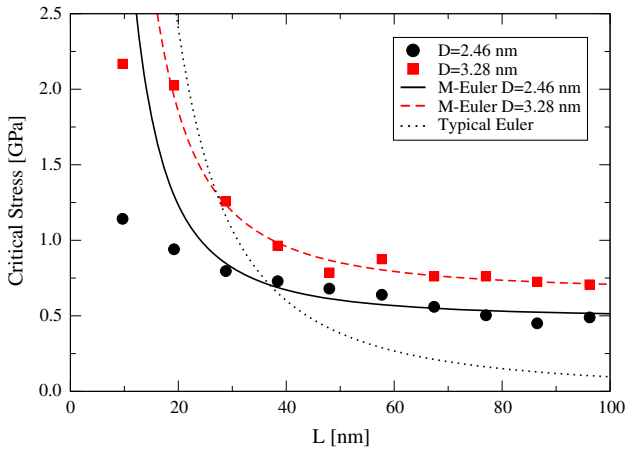

Fig. 5 Critical stress versus length for $D = 2.46$ (*circles*) and $D = 3.28$ nm (*squares*) of nanowire diameter. *Dashed line* shows the typical Euler curve

for the two diameters used. We see that in both cases the critical stress decreases with increasing slenderness following a square-type inverse law. The solid lines correspond to fitting curves according to Eq. (3). The dashed line shows the typical Euler curve, which does not consider surface effects.

It can be noticed that the fitting is good for slenderness ratios greater than 10, but it worsens for slenderness ratios lower than 10. This is not surprising since it has already been documented [18, 34] that the range of validity of the M-Euler's theory is for L/D ratios greater than 10. Lower values of slenderness naturally favor the collapse of a column by yielding.

Equation (3) and the bulk elastic modulus allow us to obtain the residual surface tension τ_0 and the surface elastic modulus E_s for each of the diameters studied. These values are summarized in Table 1. Systematic studies are needed in order to obtain the dependence between τ_0 and E_s with the diameter of the nanowire.

Table 1 Fit results, surface elastic modulus, and residual surface tension

D (nm)	E_s (eV/Å^2)	τ_0 (eV/Å^2)
2.46	−0.8501	0.0292
3.28	−1.1897	0.0532

It is interesting to note that our results are of the same order of magnitude compared with previous buckling simulations of crystalline nanowires. For example, Jiang et al. [17] studied the buckling and yielding of gold nanowires and they found a value of 35.2 GPa of elastic

modulus of nanowire by using the surface elastic modulus of -0.901 eV/Å^2 determined by Shenoy [36]. In a related work, Izumi et al. [37] studied surface effects in the critical buckling strain of silicon nanowires, obtaining $E_s = -0.807$ eV/Å^2 and $\tau_0 = -0.088$ eV/Å^2 for unreconstructed {100} silicon surfaces. Jing et al. [38] presented an experimental work on buckling in silver nanowire. They fitted values of elastic modulus versus nanowire diameter (in the range of 20–140 nm), finding values of $E_s = 0.87$ eV/Å^2 and $\tau_0 = 0.58$ eV/Å^2.

Our obtained values of E_s and τ_0 can be analyzed in terms of the analytical results deduced by He and Lilley [15] for the bending of a nanowire with fixed–fixed boundary conditions. Accordingly, $Cu_{45}Zr_{45}Al_{10}$ should have a stiffer behavior because positive values of surface stress τ_0 result in less curvature of the nanowire bending. And due to the negative value of the surface elastic modulus should these nanowires show a Young's modulus lower than the Young's modulus of a bulk sample. Other atomistic simulations, but for crystalline nanowires [13, 36], showed that E_s and τ_0 may be either positive or negative, depending on the crystallographic structure of materials. As for amorphous materials there are no privileged orientations, we expect these results reflect the buckling behavior over a wide range of metallic glasses.

Conclusions

In summary, we simulated the compression behavior and buckling in metallic glass nanowires for a set of twenty different slenderness ratios, corresponding to two nanowire diameters. We could observe from the stress–strain curves that for small strains, there exists an elastic regime and, for larger strains, buckling occurs after a certain critical stress is attained. The buckling phenomenon is accompanied by the formation of shear transformation zones that then coalesce to form shear bands. Our simulation results show good agreement with the modified theory of Euler and reinforce the fact that in the case of nanowires, the surface effects must be considered.

Acknowledgements J. Wachter acknowledges support from Conicyt D-21090391 and the National Laboratory for High Performance Computing, Chile. G. Gutiérrez and A. Zúñiga thank Fondecyt, Chile 1120603.

References

1. Johnson W (1999) Bulk glass-forming metallic alloys: science and technology. MRS Bull 24:42–56
2. Inoue A (2002) Stabilization of metallic supercooled liquid and bulk amorphous alloys. Acta Mater 48:279–306
3. Schroers J (2005) The superplastic forming of bulk metallic glasses. JOM 381:36–39
4. Schroers J, Pham Q, Peker A, Curtis RV (2007) Blow molding of bulk metallic glass. Scr Mater 57:341–344
5. Ashby M, Greer A (2003) Metallic glasses as structural materials. Scr Mater 54:321–326
6. Xia Y, Yang P, Sun Y, Wu Y, Mayers B, Gates B, Yin Y, Kim F, Yan H (2003) One-dimensional nanostructures: synthesis, characterization and applications. Adv Mater 15:353–389
7. Ekinci KL, Roukes ML (2005) Nanoelectromechanical systems. Rev Sci Instrum 76:061101
8. Wang CC, Mao YW, Shan ZW, Dao M, Li J, Jun Sun J, Evan Ma E, Suresh S (2013) Real-time, high-resolution study of nanocrystallization and fatigue cracking in a cyclically strained metallic glass. PNAS 110:19725–19730
9. Shan ZW, Li J, Cheng YQ, Minor AM, Syed SA, Warren OL, Ma E (2008) Plastic flow and failure resistance of metallic glass: insight from in situ compression of nanopillars. Phys Rev B 77:155419
10. Guo H, Yan PF, Wang YB, Tan J, Zhang ZF, Sui ML, Ma E (2007) Tensile ductility and necking of metallic glass. Nat Mater 6:735–739
11. Liang H, Upmanyu M, Huang H (2005) Size-dependent elasticity of nanowires: nonlinear effects. Phys Rev B 71:241403
12. Kulkarni AJ, Zhou M, Ke FJ (2005) Orientation and size dependence of the elastic properties of zinc oxide nanobelts. Nanotechnology 16:2749
13. Miller RE, Shenoy VB (2000) Size-dependent elastic properties of nanosized structural elements. Nanotechnology 11:139–147
14. Chen CQ, Shi Y, Zhang YS, Zhu J, Yan YJ (2006) Size dependence of Young's modulus in ZnO nanowires. Phys Rev Lett 96:075505
15. He J, Lilley CM (2008) Surface effect on the elastic behavior of static bending nanowires. Nano Lett 8:1798–1802
16. Lee HL, Chang RP, Chang WJ (2011) Buckling analysis of nonuniform nanowires under axial compression, Proceedings of the World Congress on Engineering III:2466–2468, London, UK
17. Jiang W, Batra R (2009) Molecular statics simulations of buckling and yielding of gold nanowires deformed in axial compression. Acta Mater 57:4921–4932
18. Zhan H, Gu Y (2011) Molecular dynamics study of dynamic buckling properties of nanowires with defects, 14th Asia Pacific Vib. Conf. pp 1–7
19. Olsson PAT, Park HS (2011) Atomistic study of the buckling of gold nanowires. Acta Mater 59:3883–3894
20. Yao H, Yun G (2012) The effect of nonuniform surface elasticity on buckling of ZnO nanowires. Phys E 44:1916–1919
21. Wang Y, Song J, Xiao J (2013) Surface effects on in-plane buckling of nanowires on elastomeric substrates. J Appl Phys 46:125309
22. Valencia-Balvín C, Loyola C, Osorio-Guillen J, Gutiérrez G (2010) Structural and dynamical properties of the $Cu_{46}Zr_{54}$ alloy in crystalline, amorphous and liquid state: a molecular dynamic study. Phys B 405:4970–4977
23. Cheng YQ, Ma E, Sheng HW (2009) Atomic level structure in multicomponent bulk metallic glass. Phys Rev Lett 102:245501
24. Plimpton S (1995) Fast parallel algorithms for short-range molecular dynamics. J Comp Phys 117:1–19. http://lammps.sandia.gov. Accessed 08 Aug 2014
25. Wang Z, Zu X, Gao F, Weber WJ (2008) Atomistic simulations of the mechanical properties of silicon carbide nanowires. Phys Rev B 77:224113
26. Park H, Gall K, Zimmerman J (2006) Deformation of FCC nanowires by twinning and slip. J Mech Phys Solids 54: 1862–1881

27. Riaz M, Nur O, Willander M, Klason P (2008) Buckling of ZnO nanowires under uniaxial compression. Appl Phys Lett 92:103118
28. Stukowski A (2010) Visualization and analysis of atomistic simulation data with OVITO–the Open Visualization Tool, Modelling and Simulation in Materials Science and Engineering 18:015012. http://www.ovito.org. Accessed 08 Aug 2014
29. Amigo N, Gutierrez G, Ignat M (2014) Atomistic simulation of single crystal copper nanowires under tensile stress: influence of silver impurities in the emission of dislocations. Comput Mater Sci 87:76–82
30. Shimizu F, Ogata S, Li J (2007) Theory of shear banding in metallic glasses and molecular dynamics calculations. Mater Trans 48:2923–2927
31. Wang GF, Feng XQ (2009) Surface effects on buckling of nanowires under uniaxial compression. Appl Phys Lett 94:141913
32. Wang Z, Zu X, Yang L, Gao F, Weber WJ (2008) Molecular dynamics simulation on the buckling behavior of GaN nanowires under uniaxial compression. Phys E 40:561–566
33. Wen YH, Wang Q, Liew KM, Zhu ZZ (2010) Compressive mechanical behavior of Au nanowires. Phys Lett A 374:2949–2952
34. Timoshenko SP, Gere JM (1985) Theory of elastic stability. McGraw-Hill, New York
35. Ji LW, Young SJ, Fang TH, Liu CH (2007) Buckling characterization of vertical ZnO nanowires using nanoindentation. Appl Phys Lett 90:033109
36. Shenoy V (2005) Atomistic calculations of elastic properties of metallic FCC crystal surfaces. Phys Rev B 71:094104
37. Izumi S, Hara S, Kumagai T, Sakai S (2004) A method for calculating surface stress and surface elastic constants by molecular dynamics: application to the surface of crystal and amorphous silicon. Thin Solid Films 467:253–260
38. Jing GY, Duan HL, Sun XM, Zhang ZS, Xu J, Li YD, Wang JX, Yu DP (2006) Surface effects on elastic properties of silver nanowires: contact atomic-force microscopy. Phys Rev B 73:235409